

# Asymptotic Theory of the Ponderomotive Dynamics of an Electron Driven by a Relativistically Intense Focused Electromagnetic Envelope

O.B. Shiryayev <sup>\*1,2</sup>

<sup>1</sup>Prokhorov General Physics Institute of the Russian Academy of Sciences,  
Vavilov Street 38, 117942, Moscow, Russia <http://www.gpi.ru/eng/index.php>

<sup>2</sup>Medicobiologic Faculty, N.I. Pirogov Russian National Medical Research University,  
Ostrovitianov Street 1, Box 117997, Moscow, Russia <http://rsmu.ru/3784.html>

January 31, 2019

## Abstract

A formalism for describing relativistic ponderomotive effects, which occur in the dynamics of an electron driven by a focused relativistically intense optical envelope, is established on the basis of a rigorous asymptotic expansion of the Newton and Maxwell equations in a small parameter proportional to the ratio of radiation wavelength to beam waist. The pertinent ground-state and first order solutions are generated as functions of the electron proper time with the help of the Krylov-Bogolyubov technique, the equations for the phase-averaged components of the ground state arising from the condition that the first-order solutions sustain non-secular behaviour. In the case of the scattering of a sparse electron ensemble by a relativistically intense laser pulse with an axially symmetric transverse distribution of amplitude, the resulting ponderomotive model further affords averaging over the random initial directions of the electron momenta and predicts axially symmetric electron scatter. Diagrams of the electron scatter directionality relative to the optical field propagation axis and energy spectra within selected angles are calculated from the compact ponderomotive model. The hot part of the scatter obeys a clear energy-angle dependence stemming from the adiabatic invariance inherent in the model, with smaller energies allocated to greater angular deviations from the field propagation axis, while the noise-level cold part of the scatter tends to spread almost uniformly over a wide range of angles. The allowed energy diapasons within specific angular ranges are only partially covered by the actual high-energy electron scatter.

## 1 Introduction

Interest in various aspects of the nonlinear dynamics of electrons driven by electromagnetic fields deepened with the advent of relativistic intensity laser physics, an area of study which took shape as attainable laser intensities crossed the threshold of around  $10^{19}$  W/cm<sup>2</sup> [1]. The quantity is conventionally termed the relativistic intensity. At the extreme intensities, laser pulses both induce relativistic motions of electrons born in or injected into the focal spot and have the ability to relay to them considerable post-interaction energies. The drift of an electron across the focal spot of an intense electromagnetic envelope on a timescale slow compared to the field cycle is essentially the ponderomotive effect responsible, in particular, for the net energy gain by the particle. Developing a formal description of the relativistic ponderomotive dynamics of an electron in a superstrong focused electromagnetic envelope is the purpose of the present study.

The baseline scenario behind the motions of an electron driven by the Lorentz force exerted by a relativistically intense focused envelope has been revealed in multiple simulations (e.g, see [2–8]). An

---

\*shiryayev@kapella.gpi.ru, <https://sites.google.com/site/drolegbshiryayev>

electron interacting with a relativistically intense laser pulse gets captured by the field and draws energy from it to ultimately get released with a certain residual energy. The models employed in various pertinent studies comprise relativistic Newton's equations coupled to the expressions describing the propagation of focused optical envelopes in vacuum. The formulations for the field range in complexity from those corresponding to a Gaussian transversely polarized beam with a waist to more sophisticated models embracing the corrections which account for the longitudinal component of the field [9, 10] or, furthermore, a combination of the latter with the pulse duration-related corrections to the transverse component of the field [11, 12].

The concept of ponderomotive dynamics of an electron in a high-frequency envelope can be traced back to the elegant quasilinear analysis by Gaponov and Miller [13] which reveals a ponderomotive force proportional to the gradient of the field intensity as the time-averaged driver of the electron dynamics (also, see [14]). Multiple attempts were made to generalize the ponderomotive force concept to cover the relativistic intensity range as the attainable laser intensities rose. The majority of studies replicated the approach of [13], transforming the basic equations, adopting a priori assumptions about the character of the oscillations of their various terms including the relativistic mass factor of the electron, and performing averaging in time on such basis [10, 15, 16]. An effort to implement fully the Krylov-Bogolyubov technique can be found in [17], but, in the practically important case of the linear polarization of laser radiation, the study is limited to the quasi-relativistic case due to the complexity of assessing the mode of oscillations of the electron mass factor.

An important study highlighted the crucial difference between the averaging in time and averaging over the optical field oscillation phase in exploring the dynamics of a laser-driven electron [18]. The conclusion therein is that the latter approach, representing a departure from the structural logic defined by [13] and implemented in the other studies cited above, becomes necessary if the longitudinal displacements of the field-driven particle are appreciable, which clearly is the case if the electron motion is powered by a focused intense laser pulse. The averaging attempt in terms of proper time, which is directly related to phase, was performed in [19], but the study treated the impractical and relatively simple case of circular polarization of the electromagnetic field and involved no specific field description.

Several studies detailing the ponderomotive dynamics in the one-dimensional case, corresponding to infinite focal spot size, are also available [20, 21]. It should be borne in mind that in such geometry the electron dynamics is governed by a simple invariant linking the transverse and longitudinal components of the particle momenta. An analog of such invariance being reasonably expected to manifest itself in the 3D situation [22], no theory for it is found in the above ponderomotive studies.

A formal asymptotic solution to the relativistic Newton's equation for an electron driven by the Lorentz force, which is generated by a linearly polarized intense focused optical envelope, is developed in the present paper. The small parameter for asymptotic expansion is  $\epsilon = \lambda / (2\pi w_0)$ , where  $\lambda$  and  $w_0$  are the laser pulse wavelength and waist. The role of an independent variable within the implementation of the asymptotic algorithm is assigned to the optical field phase, with the related electron fast and slow proper times being introduced. The optical field expression factoring into the Lorentz force includes high-order corrections in  $\epsilon$ , which are indispensable to the resolution of the ground-state asymptotic terms in the framework of the Krylov-Bogolyubov method. As is customary in the framework of the latter, the nonoscillatory parts of the electron coordinates and momentum emerge as integration constants in solutions to lower-order equations to be determined from the conditions that secular terms must be absent in the solutions to higher-order ones. The equations embodying this requirement ultimately provide a closed problem for the nonoscillatory variables. It can be interpreted as the corresponding set of averaged equations for the electron dynamics, though the derivation employs no explicit averaging or any a priori assumptions concerning the character of oscillations of the electron relativistic mass factor or other quantities. Importantly, the lowest-order, fully three-dimensional approximation for the laser-driven relativistic Newton's equation for an electron is shown to sustain an adiabatic invariant which appears to be analogous in shape to the well-known one found in one-dimensional geometry and, in the three-dimensional case, links the energy and the angle of motion relative to the field propagation axis for an electron ejected from the laser focal spot.

The equations resulting from the asymptotic expansion acquire a relatively compact form if the amplitude distribution of the optical field is axially symmetric. In the reduced form, the equations warrant the conclusion that, for a linearly polarized laser pulse, the scatter of an ensemble of electrons with initial momenta having a uniform angular distribution in the plane perpendicular to the laser

propagation axis also spreads uniformly over angles in the transverse plane. Solutions to the asymptotic equations describing the scattering of a sparse ensemble of electrons by relativistically intense laser radiation with axially symmetric amplitude distribution are presented below and applied to delineate the characteristics of the scatter.

## 2 Asymptotic Solutions to Relativistic Newton's Equations for a Laser-Driven Electron

The nonlinear dynamics of an electron relativistically driven by electromagnetic radiation obeys Newton's equations

$$\begin{aligned}\gamma\partial_t x &= p_x, & \gamma\partial_t y &= p_y, & \gamma\partial_t z &= p_z, \\ \partial_t \mathbf{p} &= \partial_t \mathbf{A} - \gamma^{-1}(\mathbf{p} \times (\nabla \times \mathbf{A})), & \gamma &= \sqrt{1 + \mathbf{p}^2},\end{aligned}\tag{1}$$

where  $\nabla = (\partial_x, \partial_y, \partial_z)$ ,  $\gamma$  is the relativistic mass factor, and  $\mathbf{A}$  stands for the vector potential of the field propagating in vacuum. Assuming that the field has the shape of a focused envelope, coordinates and time are normalized by the focal spot size  $w_0$  and by  $w_0/c$  respectively, and the vector potential is normalized by  $mc^2/e$ . The vector potential solves Maxwell's equations

$$\Delta \mathbf{A} - \partial_t^2 \mathbf{A} = 0, \quad (\nabla, \mathbf{A}) = 0$$

(Coulomb gauge) and, in the case of linear polarization, has the asymptotic structure represented by

$$\begin{aligned}A_x &= \exp(i\theta) \left( a(\tau, x, y, s) + \sum_{m=1}^{\infty} \epsilon^m a_{xm}(\tau, x, y, s) \right) + c.c., \\ A_y &= 0, \quad A_z = \exp(i\theta) \sum_{m=1}^{\infty} \epsilon^m a_{zm}(\tau, x, y, s) + c.c.,\end{aligned}$$

where the variables defined as  $\theta = (t - z)/\epsilon$  and  $s = \epsilon\theta$  can be interpreted as fast and slow proper times of the electron. Furthermore,  $\tau = 2\epsilon z$  and  $\epsilon = (\lambda/2\pi w_0)$ ,  $\lambda$  denoting the radiation wavelength and  $\epsilon$  being a small parameter. As shown in [12], the ground-state and first-order results for the vector potential stem from the resulting asymptotic equations

$$-4i\partial_\tau a + \Delta_\perp a = 0, \quad -4i\partial_\tau a_{x1} + \Delta_\perp a_{x1} = 4\partial_{\tau s}^2 a,$$

and are of the form

$$a(\tau, x, y, s) = a_0(s)u(x, y, \tau),\tag{3}$$

$$a_{x1}(\tau, x, y, s) = ia'_0(s)\partial_\tau(\tau u(x, y, \tau)),\tag{4}$$

$$a_{z1}(\tau, x, y, s) = -ia_0(s)\partial_x u(x, y, \tau),\tag{5}$$

where  $u(x, y, \tau)$  is the field amplitude to be calculated from the Schroedinger equation

$$-4i\partial_\tau u + \Delta_\perp u = 0$$

with  $\Delta_\perp = \partial_x^2 + \partial_y^2$ , and  $a_0(s)$  describes the laser pulse temporal profile. The simplest corresponding solution specifically treated in the concluding part of the present study portrays a Gaussian pulse

$$\begin{aligned}u(x, y, \tau) &= \frac{\Lambda(\tau, r)}{\sqrt{\tau^2 + 1}} \exp(i\psi(\tau, r)), \\ \Lambda(\tau, r) &= \exp\left(-\frac{r^2}{\tau^2 + 1}\right), \quad \psi(\tau, r) = -\frac{\tau r^2}{\tau^2 + 1} + \arctan \tau\end{aligned}$$

with  $r = \sqrt{x^2 + y^2}$  (a generalization of the above solution involving Laguerre modes in the ground state and the pertinent first-order corrections is also available [12]). The objective at hand is to develop asymptotic solutions in  $\epsilon$  to Eqs. (1)-(5), that is, to solve the relativistic electron dynamics problem under the same assumptions which yield the above envelope solutions to Maxwell equations for the field in vacuum. It should be noted that, due to the architecture of the ensuing asymptotic algorithm, the first-order corrections to the field prove necessary for obtaining even the ground-state asymptotic solutions.

Consider the electron dynamics equations (1) and (2) with the field vector potential originating from Eqs. (3)-(5). Using the obvious fact that  $\partial_t = (j/\epsilon\gamma)\partial_\theta$ , where

$$j = \gamma - p_z, \quad (6)$$

the problem is conveniently switched from  $t$  to  $\theta$  as the independent variable. To develop an asymptotic solution in  $\epsilon$ , the variables  $s$  and  $\theta$  may, in the process of cultivating the approximations, be treated as independent. The asymptotic series for the electron coordinates and momenta are

$$\begin{aligned} x(t) &= x_0(s, \theta) + \epsilon x_1(s, \theta) + \dots, & p_x(t) &= p_{x0}(s, \theta) + \epsilon p_{x1}(s, \theta) + \dots \\ y(t) &= y_0(s, \theta) + \epsilon y_1(s, \theta) + \dots, & p_y(t) &= p_{y0}(s, \theta) + \epsilon p_{y1}(s, \theta) + \dots \\ \tau(t) &= \tau_0(s, \theta) + \epsilon \tau_1(s, \theta) + \dots, & p_z(t) &= p_{z0}(s, \theta) + \epsilon p_{z1}(s, \theta) + \dots \end{aligned}$$

In this framework, the ground-state results are obtained from ordinary differential equations in  $\theta$  and found to involve arbitrary functions depending on  $s$ . These functions are to be determined based on the requirement that the solutions to higher-order equations remain free of secular growth. The ground-state solution shown below is fully nonlinear and analogous to the well-known solution to the one-dimensional problem. The higher-order equations are linear ordinary differential equations in  $\theta$ , and their solutions are explicitly spelled out in what follows with an eye to deriving non-secular behaviour conditions without unwarranted averaging assumptions. The conditions for the absence of secular growth are identifiable as the de facto averaged equations of the electron dynamics.

Denote  $m(x, y, \tau) = \text{Re } u(x, y, \tau)$  and  $n(x, y, \tau) = \text{Im } u(x, y, \tau)$ . The ground-state solutions for the coordinates and the transverse momenta, as obtained by substituting the above series into Eqs. (1)-(2) and (3)-(5), are easily integrated with the result that some of the unknowns are independent of the fast variable  $\theta$ , namely

$$x_0(s, \theta) = x_{0a}(s), \quad y_0(s, \theta) = y_{0a}(s), \quad \tau_0(s, \theta) = \tau_{0a}(s), \quad (7)$$

$$p_{x0}(s, \theta) = a_0(s) [m(x_{0a}(s), y_{0a}(s), \tau_{0a}(s)) \cos \theta - n(x_{0a}(s), y_{0a}(s), \tau_{0a}(s)) \sin \theta] + p_{x0a}(s), \quad (8)$$

$$p_{y0}(s, \theta) = p_{y0a}(s). \quad (9)$$

The functions  $x_{0a}(s)$ ,  $y_{0a}(s)$ ,  $\tau_{0a}(s)$ ,  $p_{x0a}(s)$ ,  $p_{y0a}(s)$ ,  $j_0(s)$  emerge at this point as integration constants. In a meaningful semblance to the 1D case, the above ground-state solutions show that the quantity  $j$  defined by Eq. (6), calculated to the lowest order, is independent of the fast proper time  $\theta$ , namely,

$$\gamma_0(s, \theta) - p_{z0}(s, \theta) = j_0(s), \quad (10)$$

where  $\gamma_0(s, \theta) = \sqrt{1 + p_{x0}^2(s, \theta) + p_{y0}^2(s, \theta) + p_{z0}^2(s, \theta)}$ , while  $j_0(s)$  also awaits being defined using higher-order approximations. Therefore, we have

$$p_{z0}(s, \theta) = \frac{p_{x0}(s, \theta)^2 + p_{y0}(s, \theta)^2 - j_0(s)^2 + 1}{2j_0(s)}. \quad (11)$$

Accordingly, the electron mass factor in the ground state is

$$\gamma_0(s, \theta) = \frac{p_{x0}(s, \theta)^2 + p_{y0}(s, \theta)^2 + j_0(s)^2 + 1}{2j_0(s)},$$

so that  $E = \gamma_0(s, \theta) - 1$ . In the first order, the solution to the last of Eqs. (1), rewritten for the variable  $\tau$ , evaluates to

$$\tau_1(s, \theta) = \tau_{1a}(s) - \theta \tau'_{0a}(s).$$

The above first-order solution could exhibit secular behaviour in the sense that it is a growing function of  $\theta$  and can thus become comparable in magnitude to the ground state, which runs contrary to the assumptions underlying the asymptotic approach. Obviously,  $\tau_1(s, \theta)$  stays secular-free provided that  $\tau_{0a}(s)$  in Eq. (7) is a constant, so that eventually

$$\tau_{0a}(s) = \tau_{0a}, \quad \tau_1(s, \theta) = \tau_{1a}(s).$$

Similarly, the higher-order solutions obtained below generally involve terms which grow in  $\theta$ , and, in every case, the absence of secularity requirement dictates further conditions to be imposed on the parameters of the ground-states.

The following notations are used below for brevity

$$\begin{aligned} m_0(s) &= m(x_{0a}(s), y_{0a}(s), \tau_{0a}), & n_0(s) &= n(x_{0a}(s), y_{0a}(s), \tau_{0a}), \\ m_1(s) &= \frac{\partial m(x_{0a}(s), y_{0a}(s), \tau_{0a})}{\partial x}, & n_1(s) &= \frac{\partial n(x_{0a}(s), y_{0a}(s), \tau_{0a})}{\partial x}, \\ m_2(s) &= \frac{\partial m(x_{0a}(s), y_{0a}(s), \tau_{0a})}{\partial y}, & n_2(s) &= \frac{\partial n(x_{0a}(s), y_{0a}(s), \tau_{0a})}{\partial y}, \\ m_3(s) &= \frac{\partial m(x_{0a}(s), y_{0a}(s), \tau_{0a})}{\partial \tau}, & n_3(s) &= \frac{\partial n(x_{0a}(s), y_{0a}(s), \tau_{0a})}{\partial \tau}. \end{aligned}$$

The solutions to the first-order equations for the transverse coordinates are

$$x_1(s, \theta) = \frac{a_0(s) (m_0(s) \sin \theta + n_0(s) \cos \theta)}{j_0(s)} + x_{1a}(s) + \left( \frac{p_{x0a}(s)}{j_0(s)} - x'_{0a}(s) \right) \theta, \quad (12)$$

$$y_1(s, \theta) = y_{1a}(s) + \left( \frac{p_{y0a}(s)}{j_0(s)} - y'_{0a}(s) \right) \theta. \quad (13)$$

The solutions to the first-order equations for the transverse components of the electron momentum are

$$\begin{aligned} p_{x1}(s, \theta) &= \sum_{k=1,2} (\alpha_{x,k}(s) \cos(k\theta) + \beta_{x,k}(s) \sin(k\theta)) + p_{x1a}(s) - \\ &- \left( p'_{x0a}(s) + \frac{a_0^2(s) (m_0(s)m_1(s) + n_0(s)n_1(s))}{2j_0(s)} \right) \theta, \end{aligned} \quad (14)$$

$$\begin{aligned} p_{y1}(s, \theta) &= \sum_{k=1,2} (\alpha_{y,k}(s) \cos(k\theta) + \beta_{y,k}(s) \sin(k\theta)) + p_{y1a}(s) - \\ &- \left( p'_{y0a}(s) + \frac{a_0^2(s) (m_0(s)m_2(s) + n_0(s)n_2(s))}{2j_0(s)} \right) \theta, \end{aligned} \quad (15)$$

where the coefficients of the oscillatory parts are

$$\alpha_{x,1}(s) = a_0(s) \left( -\frac{n_1(s)p_{x0a}(s)}{j_0(s)} + m_1(s)x_{1a}(s) + m_2(s)y_{1a}(s) + m_3(s)\tau_{1a}(s) \right) - a'_0(s) (n_0(s) + n_3(s)\tau_{0a}),$$

$$\alpha_{x,2}(s) = a_0^2(s) \frac{m_0(s)n_1(s) + n_0(s)m_1(s)}{4j_0(s)},$$

$$\beta_{x,1}(s) = -a_0(s) \left( \frac{m_1(s)p_{x0a}(s)}{j_0(s)} + n_1(s)x_{1a}(s) + n_2(s)y_{1a}(s) + n_3(s)\tau_{1a}(s) \right) - a'_0(s) (m_0(s) + m_3(s)\tau_{0a}),$$

$$\beta_{x,2}(s) = a_0^2(s) \frac{m_0(s)m_1(s) - n_0(s)n_1(s)}{4j_0(s)},$$

$$\begin{aligned}\alpha_{y,1}(s) &= -a_0(s) \frac{n_2(s)p_{x1a}(s)}{j_0(s)}, & \alpha_{y,2}(s) &= -a_0^2(s) \frac{n_0(s)m_2(s) + m_0(s)n_2(s)}{4j_0(s)}, \\ \beta_{y,1}(s) &= -a_0(s) \frac{m_2(s)p_{x1a}(s)}{j_0(s)}, & \beta_{y,2}(s) &= a_0^2(s) \frac{n_0(s)n_2(s) - m_0(s)m_2(s)}{4j_0(s)}.\end{aligned}$$

The second-order equation for the longitudinal coordinate is given by

$$\begin{aligned}\tau_2(s, \theta) &= \sum_{1,2} [\sigma_k(s) \cos(k\theta) + \delta_k(s) \sin(k\theta)] + \tau_{2a}(s) + \\ &+ \left[ \frac{2(p_{x0a}(s)^2 + p_{y0a}(s)^2 + 1) + a_0^2(s)(m_0(s)^2 + n_0(s)^2)}{2j_0(s)^2} - \tau'_{1a}(s) - 1 \right] \theta, \quad (16)\end{aligned}$$

where the coefficients of the oscillatory part are

$$\begin{aligned}\sigma_1(s) &= \frac{2a_0(s)n_0(s)p_{x0a}(s)}{j_0^2(s)}, & \sigma_2(s) &= \frac{a_0^2(s)n_0(s)m_0(s)}{2j_0^2(s)}, \\ \delta_1(s) &= \frac{2a_0(s)m_0(s)p_{x0a}(s)}{j_0^2(s)}, & \delta_2(s) &= \frac{a_0^2(s)[m_0^2(s) - n_0^2(s)]}{2j_0^2(s)},\end{aligned}$$

The longitudinal momentum is found to be

$$\begin{aligned}p_{z1}(s, \theta) &= \frac{p_{x0}(s, \theta)p_{x1}(s, \theta) + p_{y0}(s, \theta)p_{y1}(s, \theta)}{j_0(s)} + \\ &+ \frac{\gamma_0(s, \theta) [\Pi(s)j_0(s) + a_0(s)(m_1(s) \sin \theta + n_1(s) \cos \theta)]}{j_0(s)} + \theta j'_0(s)/j_0(s).\end{aligned} \quad (17)$$

The functions  $x_{1a}(s)$ ,  $y_{1a}(s)$ ,  $p_{x1a}(s)$ ,  $p_{y1a}(s)$ ,  $\tau_{2a}(s)$ , and  $\Pi(s)$  would have to be calculated from higher-order equations, but the non-secular behaviour conditions necessary to completely define the ground-state can be drawn from Eqs. (12)-(17). The prerequisites obviously read

$$p_{x0a}(s) = j_0(s)x'_{0a}(s), \quad p_{y0a}(s) = j_0(s)y'_{0a}(s) \quad (18)$$

$$p'_{x0a}(s) = -\frac{a_0^2(s)(m_0(s)m_1(s) + n_0(s)n_1(s))}{2j_0(s)}, \quad (19)$$

$$p'_{y0a}(s) = -\frac{a_0^2(s)(m_0(s)m_2(s) + n_0(s)n_2(s))}{2j_0(s)}, \quad (20)$$

$$j_0(s) = \text{const}, \quad (21)$$

$$\tau'_{1a}(s) = \frac{a_0^2(s)(m_0^2(s) + n_0^2(s)) + 2(p_{x0a}^2(s) + p_{y0a}^2(s) + 1 - j_0^2(s))}{2j_0^2(s)}. \quad (22)$$

Eqs. (19) and (20) can be cast in the form

$$p'_{x0a}(s) + \frac{a_0^2(s)}{2j_0} \partial_x W(x_{0a}(s), y_{0a}(s), \tau_{0a}) = 0, \quad (23)$$

$$p'_{y0a}(s) + \frac{a_0^2(s)}{2j_0} \partial_y W(x_{0a}(s), y_{0a}(s), \tau_{0a}) = 0, \quad (24)$$

$$W(x, y, \tau) = \frac{m^2(x, y, \tau) + n^2(x, y, \tau)}{2} = \frac{|u(x, y, \tau)|^2}{2}, \quad (25)$$

meaning that  $W_p(x, y, \tau, s) = a_0^2(s)W(x, y, \tau)$  plays the role of the ponderomotive potential of the original system. Eqs. (18)-(21), (23), and (24) represent the ponderomotive dynamics problem for an electron in the relativistic case and a rigorous generalization of the classic result of [13].

### 3 Averaged Dynamics in Cylindrical Coordinates

Consider Eqs. (18)-(21) in cylindrical coordinates, the transition being introduced by  $x_{0a}(s) = r(s) \cos(\varphi(s))$ ,  $y_{0a}(s) = r(s) \sin(\varphi(s))$ ,  $p_{x0a}(s) = \rho(s) \cos(\psi(s))$ ,  $p_{y0a}(s) = \rho(s) \sin(\psi(s))$ . Further denote  $\delta\psi(s) = \varphi(s) - \psi(s)$  and

$$W(x, y, \tau) = c(r^2, \varphi, \tau_{0a}).$$

Eqs. (18)-(21) thereby translate into

$$\begin{aligned} r'(s) &= \frac{\rho(s) \cos(\delta\psi(s))}{j_0}, \\ \rho'(s) &= \frac{a_0^2(s)}{4j_0 r(s)} \left[ \sin(\delta\psi(s)) \partial_\varphi c(r^2(s), \varphi(s), \tau_{0a}) - 2 \cos(\delta\psi(s)) r^2(s) \frac{\partial c(r^2(s), \varphi(s), \tau_{0a})}{\partial r^2} \right], \\ \varphi'(s) &= -\frac{\sin(\delta\psi(s)) \rho(s)}{j_0 r(s)}, \\ \psi'(s) &= -\frac{a_0^2(s)}{4j_0 r(s) \rho(s)} \left[ \cos(\delta\psi(s)) \frac{\partial c(r^2(s), \varphi(s), \tau_{0a})}{\partial \varphi} + 2 \sin(\delta\psi(s)) r^2(s) \frac{\partial c(r^2(s), \varphi(s), \tau_{0a})}{\partial r^2} \right]. \end{aligned} \quad (26)$$

The equations in the cylindrical coordinate frame further allow for a reduction to a problem with three unknowns instead of four if the field intensity is axially symmetric. In this case, we denote  $c(r^2, \varphi, \tau_{0a}) = c_0(r^2, \tau_{0a})$  and arrive at a set of electron dynamics equations comprising Eq. (26) and

$$\rho'(s) = -\frac{a_0^2(s) r(s) \cos(\delta\psi(s)) \frac{\partial}{\partial r^2} c_0(r^2(s), \tau_{0a})}{2j_0}, \quad (27)$$

$$\delta\psi'(s) = \frac{\sin \delta\psi(s) \left[ a_0^2(s) r^2(s) \frac{\partial c_0(r^2(s), \tau_{0a})}{\partial r^2} - 2\rho^2(s) \right]}{2j_0 r(s) \rho(s)}. \quad (28)$$

In particular,  $c_0(r^2, \tau_{0a}) = \exp[-2r^2/(\tau_{0a}^2 + 1)] / (\tau_{0a}^2 + 1)$  for a Gaussian pulse.

In what follows, the model for the laser pulse longitudinal profile is  $a_0(s) = q \exp[-(s-d)^2/\sigma^2]$ , where  $q$  is the pulse peak amplitude,  $\sigma$  is the pulse duration, and  $d$  is the distance between the pulse peak and the initial coordinate of the electron.

### 4 Ponderomotive Symmetry Breaking in an Intense Optical Field

Considering the interaction of the optical field with a sufficiently sparse target consisting of a large number of electrons, it is natural to assume that the electrons sustain unidirectionally random motion prior to the target's being overrun by the propagating electromagnetic pulse. In this case, the initial values of momentum angle  $\psi$  uniformly span the whole range from 0 to  $2\pi$  for every initial value of the coordinate angle  $\varphi$ . Therefore, the scattering of the above ensemble is axially symmetric, and Eqs. (26)-(28) should be treated for consecutive values of  $\delta\psi$  similarly varying over the full angular difference range. Two representative cases of the electron scattering by a laser pulse are shown below. In the first one, depicted in Fig. 1, the laser radiation disperses a target initially located at a large distance from the pulse peak. The scattering occurs chiefly at the pulse front, which explains the electron energy outputs appearing to be modest against the ultrarelativistic laser intensity (note that this circumstance was observed both in experiments and in prior simulations based on direct solution of the electron dynamics equations [12, 23]). In the second case, illustrated in Fig. 2, the electrons are initially placed within the domain occupied by the optical field as in the case of the ionization self-injection [24, 25] (no attempt is made in this study to simulate the ionization dynamics consistent with the laser field). Under the

arrangement, the electrons exposed to the central part of the laser pulse are released with much higher energies than in the case shown in Fig. 1. The initial conditions in all calculations are formulated so that electrons take off with relatively small random momenta which correspond to the adiabatic invariant  $j_0$  exhibiting slight random deviations from unity.

The paradigm exemplified by both cases is the symmetry breaking in the dynamics of the electrons driven by the transversely localized optical field. The phase difference  $\delta\psi$  vanishes quickly and the ponderomotively pressured electron gains momentum on the average to be, in the long run, ejected from the interaction zone. Calculations demonstrate that the release of electrons covered by the focal spot, as evidenced by Figs. 1 and 2, occurs almost exactly at the focal spot edge defined by  $(r(s)/\sqrt{1+\tau^2}) = 1$ . The electron ejection angle inferred from Eqs. (6) and (11) is expressed as  $\theta_{\text{eject}} = \tan^{-1} [2j_0\rho / (1 + \rho^2 - j_0^2)]$ .

The scattering of an ensemble of electrons is further examined on the basis of the proposed theory. The energy-directionality diagram for the same optical field parameters as in the case of Fig. 1 is presented in Fig. 3. The numbers of electrons within specific ranges of angles relative to the field propagation direction are displayed, with the angles expressed in terms of their energy equivalents as prescribed by Eq. (11) and the ensuing expressions for the relativistic mass factor and energy. Sub-ponderomotive noise, i.e. the energies having magnitudes which border on the precision of the asymptotic method employed, are filtered from the plot. Fig. 4 demonstrates in detail two representative energy spectra resulting from the scattering of electrons into specific angular ranges. An energy-directionality diagram and two representative electron energy spectra for the field parameters of Fig. 2 are shown in Figs. 5 and 6 respectively.

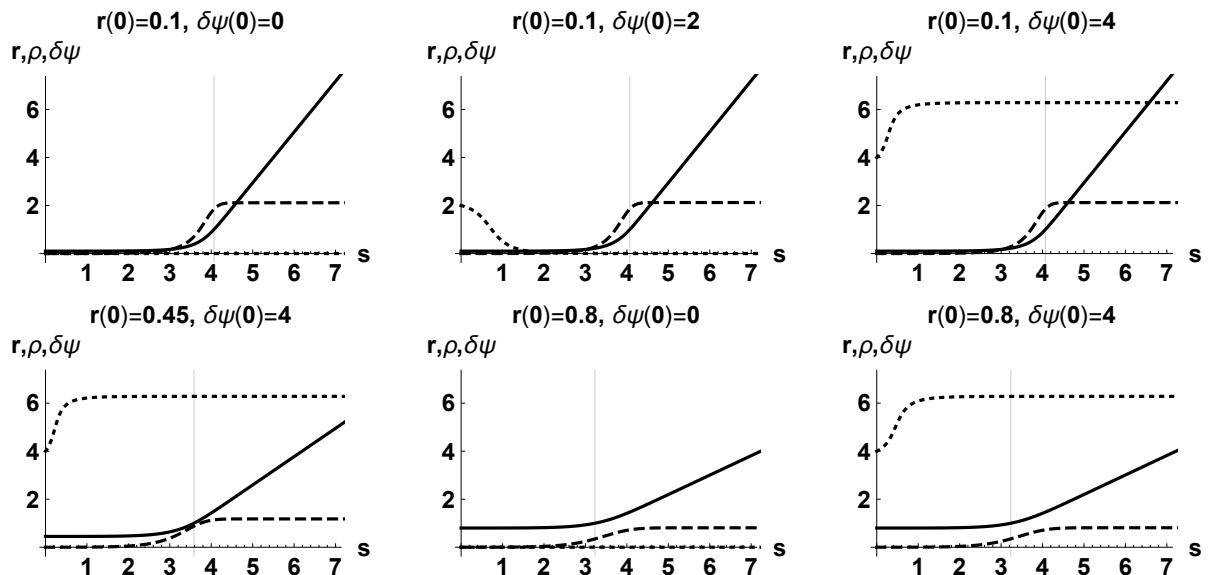


Figure 1: Averaged radial coordinate  $r(s)$  (continuous line), radial component of momentum  $\rho(s)$  (dashed line), and phase difference between coordinate and momentum  $\delta\psi(s)$  (dotted line) for an electron driven by a relativistically intense focused optical envelope. The optical field parameters are  $q = 33$ ,  $\sigma = 4$ ,  $d = 10$  (interaction with a distant target). Computation results are shown for  $\tau_{0a} = 0$  (focal plane) and a range of initial positions of an electron in this plane. The envelope small parameter is  $\epsilon = 0.1$ . The initial electron momenta are generated as random values on the order of 0.1% of the relativistic threshold (the adiabatic invariant fluctuates from case to case accordingly). The results are depicted in proper time and show clearly the steady gain of energy on the average by the electron and the ultimate release of the electron from the state of being captured by the field due to the symmetry breaking in the focused electromagnetic envelope.



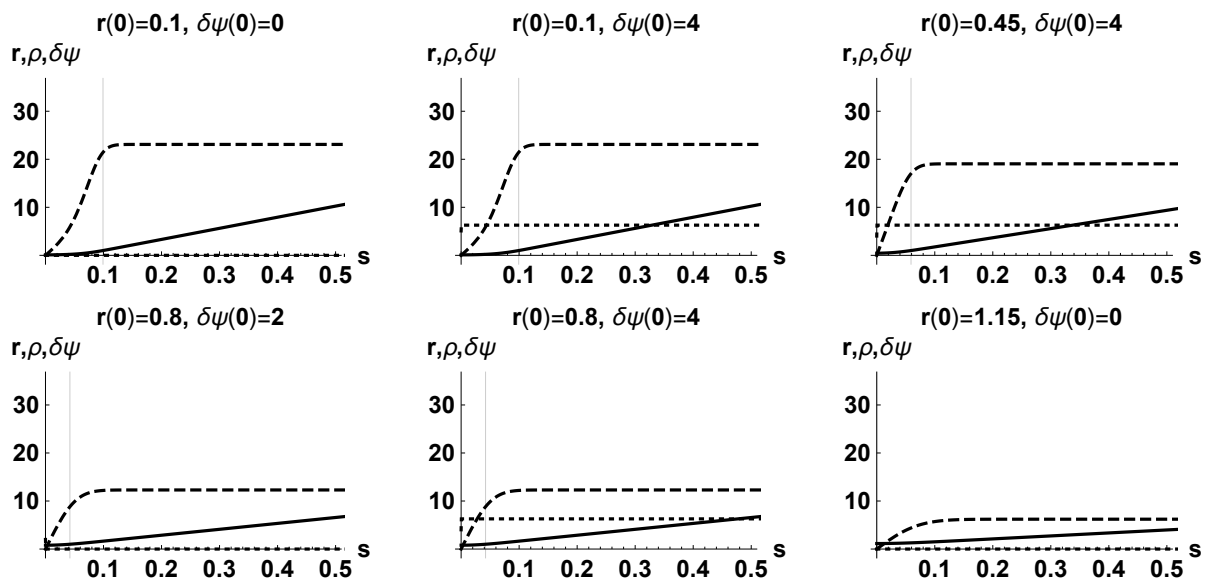


Figure 2: Averaged radial coordinate  $r(s)$  (continuous line), radial component of momentum  $\rho(s)$  (dashed line), and phase difference between coordinate and momentum  $\delta\psi(s)$  (dotted line) for an electron driven by a relativistically intense focused optical envelope. The optical field parameters are  $q = 33$ ,  $\sigma = 4$ ,  $d = 0$  (self-injection). Computation results are shown for  $\tau_{0a} = 0$  (focal plane) and a range of initial positions of an electron in this plane. The envelope small parameter is  $\epsilon = 0.1$ . The initial electron momenta are generated as random values on the order of 0.1% of the relativistic threshold (the adiabatic invariant fluctuates from case to case accordingly). The results are depicted in proper time and show clearly the steady gain of energy on the average by the electron and the ultimate release of the electron from the state of being captured by the field due to the symmetry breaking in the focused electromagnetic envelope.

## 5 Conclusions

A rigorous asymptotic approach is employed to describe the relativistic ponderomotive effects in the dynamics of an electron driven by an intense focused finite-duration electromagnetic envelope, the expansion parameter being proportional to the ratio of the field wavelength to the focal spot size. The resulting theory of ponderomotive dynamics is further applied to model the scattering of a sparse ensemble of electrons by a relativistically intense laser pulse. A refined set of electromagnetic field equations is suggested to consistently account for the envelope shape, the longitudinal component of the propagating pulse, and the field corrections due to finite-duration effects. Approximate solutions to the relativistic equations of the electron dynamics are generated with the help of the Krylov-Bogolyubov technique which leads to a set of equations de facto averaged over field oscillations and written in terms of the proper time of the electron, as well as to the establishment of an adiabatic invariant linking the param-

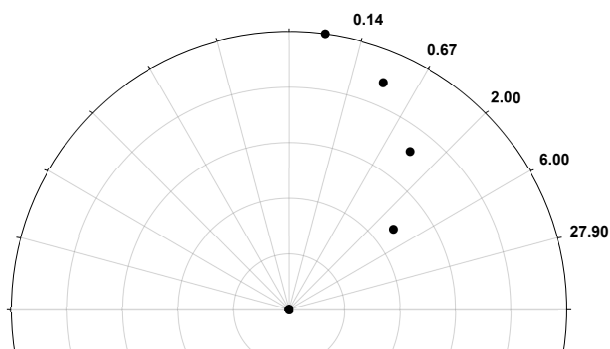


Figure 3: Diagrams of electron scatter directionality relative to the optical field propagation axis for the optical field parameters cited in Fig. 1. The sub-ponderomotive noise is filtered out and the angles are expressed in terms of the electron energy estimates based on the adiabatic invariant with  $j_0 = 1$ . The actual electron energies may spread slightly across the limits shown due to individual fluctuations of the value of  $j_0$  per individual particle, while electrons with some of the energies marginally fitting into the specified energy ranges may be absent.

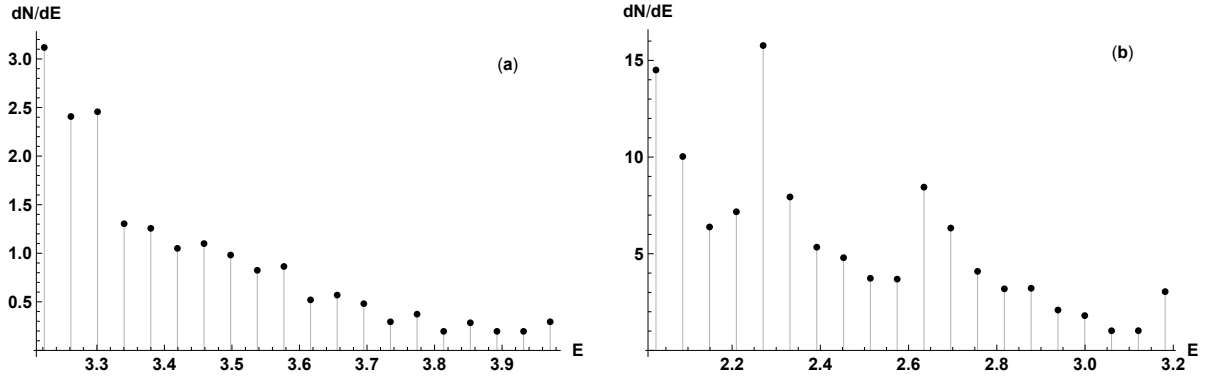


Figure 4: Electron release energies for the optical field parameters cited in Fig. 1. (a) Electron scatter energy spectrum for  $0.59 \leq \theta \leq 0.67$ . (b) Electron scatter energy spectrum for  $0.67 \leq \theta \leq 0.79$ .

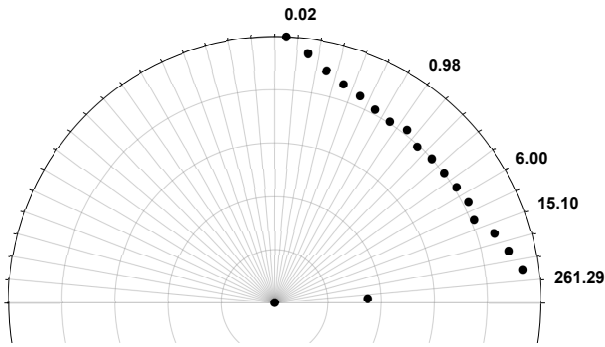


Figure 5: Diagrams of electron scatter directionality relative to the optical field propagation axis for the optical field parameters cited in Fig. 2. The subponderomotive noise is filtered out and the angles are expressed in terms of the electron energy estimates based on the adiabatic invariant with  $j_0 = 1$ . The actual electron energies may spread slightly across the limits shown due to individual fluctuations of the value of  $j_0$  per individual particle, while electrons with some of the energies marginally fitting into the specified energy ranges may be absent.

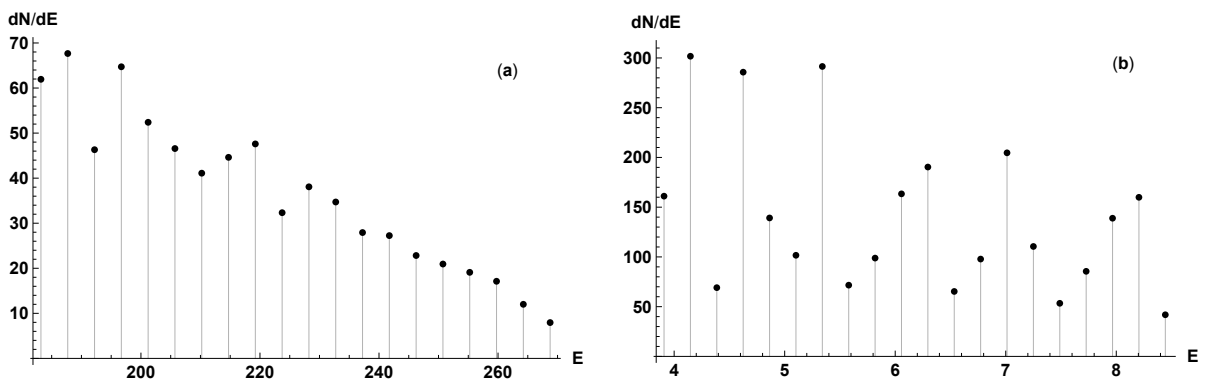


Figure 6: Electron release energies for the optical field parameters cited in Fig. 2. (a) Electron scatter energy spectrum for  $0.08 \leq \theta \leq 0.1$ . (b) Electron scatter energy spectrum for  $0.45 \leq \theta \leq 0.63$ .

ters of the post-interaction motion picture for an electron in proper time to its ejection angle and release energy in the original reference frame. For pulses with axially symmetric intensity profiles, the relativistic ponderomotive equations are found to be reducible to a form which immediately affords averaging out the random angular dependencies in initial conditions for the electron ensemble. Electron scatter directionality diagrams and energy spectra within selected angles are calculated from the resulting compact model.

## References

- [1] G.A. Mourou, T. Tajima, S.V. Bulanov, *Rev. Mod. Physics* **78**, 309 (2006)
- [2] J. X. Wang, Y. K. Ho, Q. Kong, L.J. Zhu, L. Feng, S. Scheid, and H. Hora, *Phys. Rev. E* **58**, 6575 (1998)
- [3] Q. Kong, Y.K. Ho, J.X. Wang, P.X. Wang, L. Feng, Z.S. Yuan, *Phys. Rev. E* **61**, 1981 (2000)
- [4] P.X. Wang, Y.K. Ho, X.Q. Yuan, Q. Kong, N. Cao, A. M. Sessler, E. Esarey, and Y. Nishida, *Appl. Phys. Lett.* **78**, 2253 (2001)
- [5] N. Cao, Y.K. Ho, P.X. Wang, J. Pang, Q. Kong, L. Shao, and Q.S. Wang, *J. Appl. Phys.* **92**, 5581 (2002)
- [6] J. Pang, Y.K. Ho, X.Q. Yuan, N. Cao, Q. Kong, P.X. Wang, L. Shao, E.H. Esarey, and A.M. Sessler, *Phys. Rev. E* **66**, 066501 (2002)
- [7] Y.I. Salamin, G.R. Mocken, and C.H. Keitel, *Phys. Rev. E ST - Accel.Beams* **5**, 101301 (2002)
- [8] A.L. Galkin, M.P. Kalashnikov, V.K. Klinkov, V.V. Korobkin, M.Yu. Romanovsky, and O.B. Shiryaev, *Phys. Plasmas* **17**, 053105 (2010)
- [9] M. Lax, W.H. Louissel, W.B. McKnight, *Phys. Rev. A* **11**, 1365 (1975)
- [10] B. Quesnel, P. Mora, *Phys. Rev. E* **58**, 3719 (1998)
- [11] V.P. Milant'ev, S.P. Karnilovich, Ya.N. Shaar, *Quantum Electronics* **45** (11) 1063 (2015)
- [12] O.B. Shiryaev, *Laser and Particle Beams* **35**, 64 (2017)
- [13] A.V. Gaponov, M.A. Miller, *Sov. Phys. JETP* **7**, 515 (1958)
- [14] T.W.B. Kibble, *Phys. Rev.* **150**, 1060 (1966)
- [15] V. D. Taranukhin, *JETP* **90**, 447 (2000)
- [16] A.V. Serov, *JETP* **92**, 20 (2001)
- [17] V.P. Milant'ev, A.J. Castillo, *J. Exp. Theor. Phys.* **116**, 558 (2013)
- [18] M.D. Tokman, *Plasma Physics Reports* **25**, 140 (1999)
- [19] N. B. Narozhny, M. S. Fofanov, *JETP* **90**, 753 (2000)
- [20] I.Y. Dodin, N.J. Fisch, and G.M. Fraiman, *JETP Lett.* **78**, 238 (2003)
- [21] I.Y. Dodin, N.J. Fisch, *Phys. Rev. E* **68**, 056402 (2003)
- [22] F.V. Hartemann, J.R. Van Meter, A.L. Troha, E.C. Landahl, N.C. Luhmann, Jr., H.A. Baldis, Atul Gupta, and A.K. Kerman, *Phys. Rev. E* **58**, 5001 (1998)
- [23] M. Kalashnikov, A. Andreev, K. Ivanov, A. Galkin, V. Korobkin, M. Romanovsky, O. Shiryaev, M. Schnuerer, J. Braenzel, V. Trofimov, *Laser and Particle Beams* **33**, 361 (2015)
- [24] S. X. Hu and Anthony F. Starace, *Phys. Rev. Lett.* **88**, 245003 (2002)
- [25] S.X. Hu and Anthony, F. Starace, *Phys. Rev. E* **73**, 066502 (2006)